HARD PHOTON INTERFEROMETRY IN HEAVY ION COLLISIONS*

Y. SCHUTZ

GANIL
BP 5027, 14021 Caen, France

(Received Ocotber 15, 1993)

It is shown how first- and second-order interference effects can be used to measure the extent of chaotic light sources such as stars viewed from a great distance. The same technique can be applied in nuclear physics where the interference effect arises from the quantum statistics of identical particles. The results from an experiment attempting to measure the size of the participant zone in a heavy-ion reaction using bremsstrahlung photons as a probe are presented.

PACS numbers: 25.70. -z

1. Introduction

The observation by Young at the beginning of the XIX century of intensity fringes when the values of the electromagnetic field at two distant points are superposed, as in the two-slit experiment, provided the irrefutable proof for the wave nature of light. Later the same interference effects were shown to occur for massive particles thus demonstrating the dual nature of quantum objects. This kind of interference, which is now called first-order or amplitude interference, was interpreted by Dirac [1] as the interference of a particle with itself. This interpretation was demonstrated [2] to be true in experiments where only one particle at a time was present in the interferometer. The interference fringes for electrons could be observed under conditions where the mean interval between successive electrons was about 150 km – the interferometer being only 1.5 m long!

The observation of fringe blurring was used in Michelson type of interferometers to measure the angular dimension of stars. The resolution of this

* Presented at the XXIII Mazurian Lakes Summer School on Nuclear Physics, Piaski, Poland, August 18-28, 1993.

apparatus is however limited because of the difficulties to keep the relative phase of the interferring field at two distant locations constant. In 1954, Hanbury-Brown and Twiss [3] developed a new type of interferometer for use in radio-astronomy where they showed that different photons can also interfere, in apparent contradiction with the self-interference interpretation. The distinction between this interference process, called second order or intensity interference, and Young's two-slit interference phenomenon is that the former is a multiparticle process peculiar to quantum mechanics where the notion of *different* particles must be redefined.

In the sixties, the intensity interferometry was applied to particle physics by measuring the correlation between identical particles [4]. In that way it became possible to measure the size of the pion source in antiproton-proton annihilation reactions. In nuclear physics [5], at energies close to the Fermi energy, correlations between identical nucleons or light composite particles were used but without ever observing the interference effects, obscured by final state interactions between the two particles.

I will present here a pioneering experiment where the correlation between photons has been measured to search for the intensity interference effect and thus determine the extent of the source emitting these photons.

In the first two sections I will recall under which conditions the interference pattern arises both in first and second order interference experiments. I will also show how the disappearance of the pattern can be used to measure the size of the light source. I will then briefly review what we know about the mechanism producing hard photons in heavy-ion reactions and show that these photons are well suited for the observation of the intensity interference effect. Finally, the method employed to measure the two-photon correlation will be presented together with the results we have obtained in the reaction Kr+Ni at 60 MeV/u.

2. Amplitude or first order interference

We define interference as the superposition of the electromagnetic field evaluated at two points separated in space and time. Such a superposition can be achieved with the set-up shown in Fig. 1. Two identical pinholes located at r_1 and r_2 on a first screen $E1$ are illuminated by two independent chaotic light sources. At a distance D the superposition of the light from the two pinholes is observed on a second screen $E2$. The light, which we shall assume to be monochromatic and linearly polarized, can be described by its electric field. At a time t and a position R, the observed intensity on $E2$ results from the linear superposition of the fields at r_1 and r_2 at earlier times determined by the velocity of light:

$$I(R,t) = |E(r_1,t_1) + E(r_2,t_2)|^2 \ ,$$

$$t_i = d_i/c\,,$$
$$d_i = |R - r_i| \quad i = 1,2\,. \tag{1}$$

If we write the electric field as a plane wave,

$$E(r,t) = E_0 \exp\left\{ i\left[kr - \omega t + \Phi(t)\right]\right\},$$

expression (1) becomes:

$$I(R,t) = 2E_0^2\left\{1 + \cos\left[k\left(d_1 - d_2\right) + \Phi_1(t) - \Phi_2(t)\right]\right\}. \tag{2}$$

For chaotic light sources the coherence time, t_c, is defined as the time during which the phase of the electromagnetic field remains approximately constant. In other words, the coherence time is a characteristic time for the source which determines the time scale of the random fluctuations. It is of the order of 10^{-11} seconds for a discharge lamp and 10^{-6} seconds for a laser. The path length, $l_c = ct_c$, associated with the coherence time is known as the coherence length.

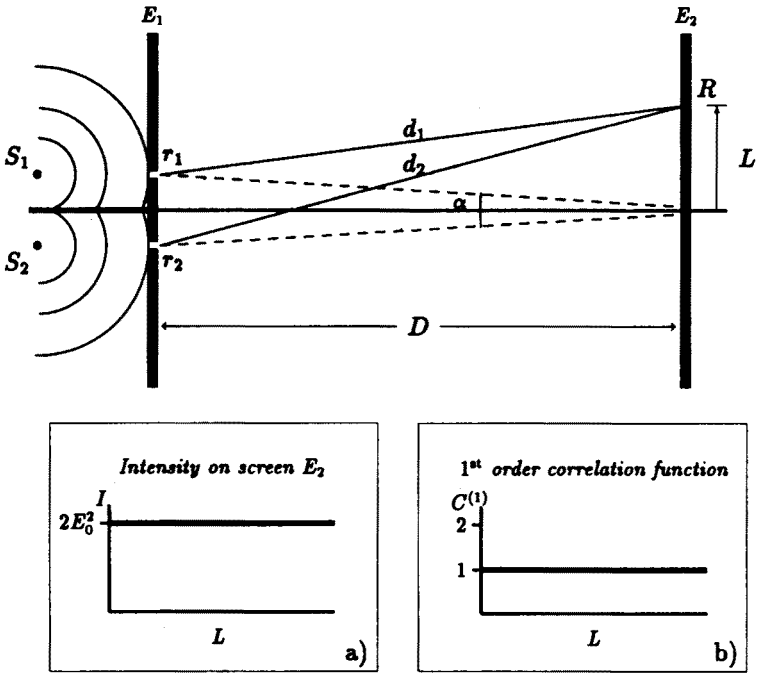

Fig. 1. Schematic set-up allowing the superposition of the electromagnetic field at two locations r_i and r_j. The sources S_1 and S_2 are independent therefore (a) no interference fringes are observed on $E2$ and (b) the correlation function is equal to 1.

The intensity is normally recorded by photographic plates or is observed with the naked eye. In either case, the recording time T is long compared to the coherence time. The observed intensity is therefore a time-average of the intensity:

$$I(R) = \overline{I(R,t)} = \frac{1}{T}\int_0^T I(R,t)\,dt\,. \tag{3}$$

Since the two sources are chaotic and independent, the phases of the field at r_i and r_j fluctuate randomly and the second term of Eq. (2) is zero on average. The averaged intensity is thus constant and equal to $2E_0^2$ and therefore the screen E_2 is uniformly illuminated.

To keep the relative phase $\delta(t)$ constant, Young changed the set-up of Fig. 1 so that the two pinholes are illuminated by a single light source positioned at an equal distance from r_1 and r_2. Such a set-up is shown in Fig. 2. If we take $\delta(t) = \text{constant} = 0$ the observed intensity is:

$$I(R) = 2E_0^2\left\{1 + \cos\left[k\,(d_1 - d_2)\right]\right\}. \tag{4}$$

It consists of two contributions. The first term represents the intensities due to each of the pinholes in the absence of the other. This term does not cause the interference effects. The fringes are described by the second term which includes the correlation function for the field at the two pinholes. The fringe pattern depends on the path difference $d_1 - d_2$ and the visibility of the fringes can be represented by the first order correlation function defined as:

$$C^{(1)}(R) = \frac{I_{r_1 r_2}(R)}{\left[I_{r_1}(R)\,I_{r_2}(R)\right]^{1/2}}\,. \tag{5}$$

For the set-up of Fig. 1, the first order correlation function is equal to 1 (no fringe visibility) and for the set-up of Fig. 2 it is equal to (using the notations of Fig. 2):

$$\begin{aligned} C^{(1)}(L) &= 1 + \cos\left[k\,(d_1 - d_2)\right] \\ &= 1 + \cos\left(k\alpha L\right)\,. \end{aligned} \tag{6}$$

The finite extent of the source in the direction joining the pinholes, neglected in the above treatment, is often the most important limiting factor for the fringe visibility. The most brilliant fringe is at the center of the screen $R = 0$, and the intensity of a fringe will decrease when one moves away from the center. The fringes will disappear altogether when the path difference exceeds the coherence length. There are actually techniques for determining the angular diameter of distant light sources, for example stars,

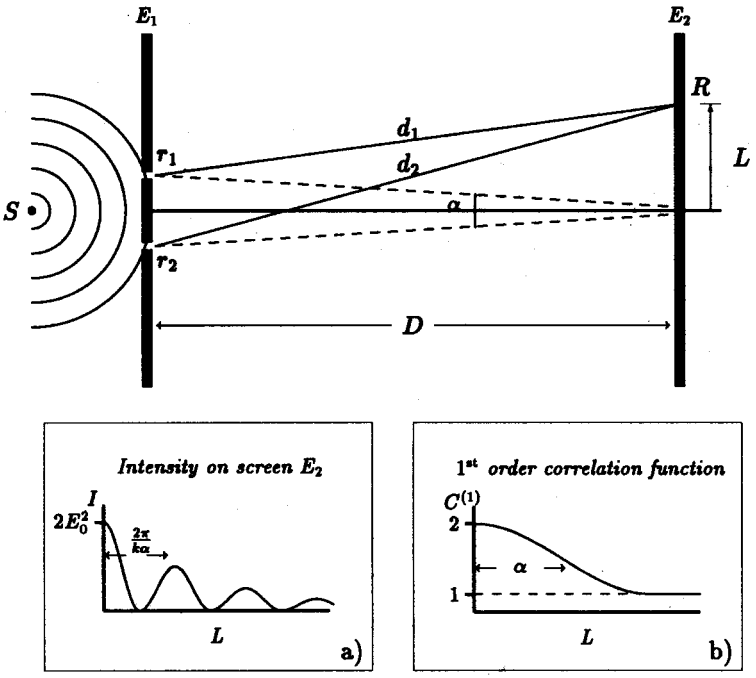

Fig. 2. Schematic set-up for the coherent superposition of the electromagnetic field at two locations r_i and r_j: a) interference fringes are observed on $E2$ and b) the correlation function has a maximum at the center (maximum fringe visibility) and decreases at large L where the fringes become difficult to observe.

by observation of fringe blurring. This can be achieved with the Michelson interferometer schematized in Fig. 3 where the star, a disk of radius R, is viewed by two aerials in which currents are summed through two cables of equal length $L/2$.

The contribution I_i to the summed intensity from one atom at r_i is, according to Eq. (4):

$$I_i(L) = 2E_0^2\left\{1 + \cos\left(k\alpha_i L\right)\right\} \tag{7}$$

and the total intensity I_Σ for N atoms distributed according to a normalized density distribution $\rho(r_i)$ is:

$$\begin{aligned} I_\Sigma(L) &= \int_{\text{source}} I_i(L)\rho(r_i)\, dr_i \\ &= 2NE_0^2\left\{1 + (N-1)\left|\tilde{\rho}(k\alpha L)\right|^2\right\}, \end{aligned} \tag{8}$$

where $\tilde{\rho}$ is the Fourier transform of the density distribution and $\alpha = R/D$ is the angular dimension of the source viewed from the distance D. The first

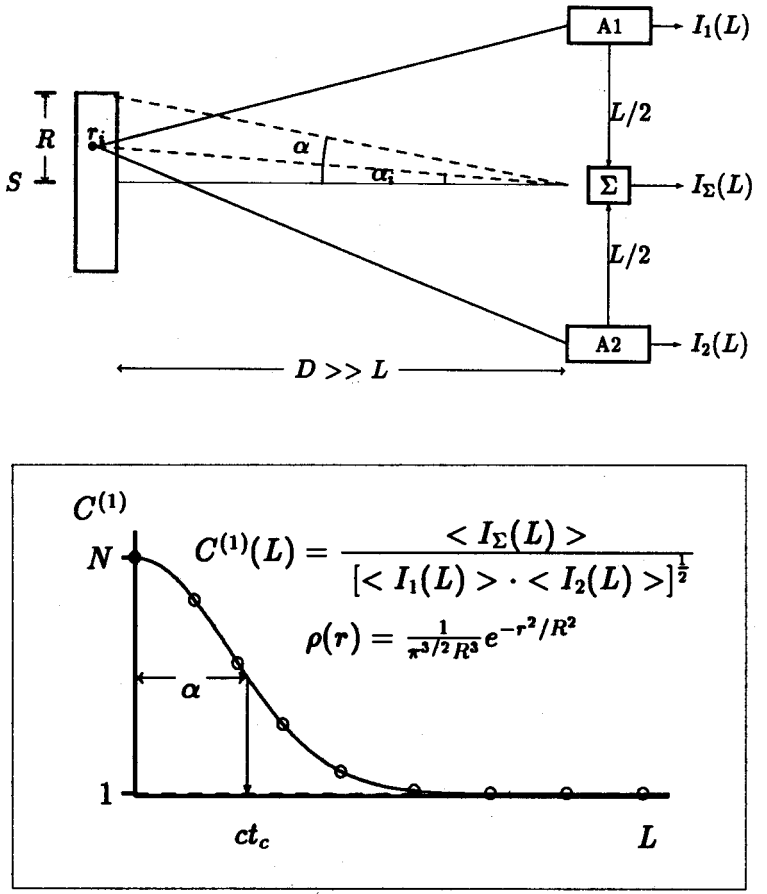

Fig. 3. Schematic set-up of the Michelson interferometer and expected correlation function for a Gaussian density distribution

order correlation function has the following form:

$$C^{(1)}(L) = 1 + |\tilde{\rho}(k\alpha L)|^2 \ . \tag{9}$$

The correlation function is measured from $L = 0$ up to distances exceeding the spatial coherence length and the observed fall off (see Fig. 3) measures the angular radius of the star.

The difficulty and the resolution limitation of this kind of interferometer originate from the necessity to keep the relative phase constant during the measurement. This is rather difficult to achieve because of phase fluctuations due to atmospheric turbulences or phase shifts along the cables. To avoid this constraint, Hanbury-Brown and Twiss introduced in 1954 [3] a new concept and developed the intensity interferometer.

3. Intensity or second order interference

The aerials can be replaced by photomultipliers and instead of summing the outputs as for the Michelson interferometer, the Intensity interferometer, schematized in Fig. 4, measures the coincidence rate. It, therefore, allows one to measure the correlation of two intensities at different times and locations rather than as previously the correlation of the electric field. One defines the second order correlation function as the ratio of the coincidence rates and the product of the single rates:

$$C^{(2)}(R_1, R_2) = \frac{I_{\Pi}(R_1, R_2)}{I(R_1) \cdot I(R_2)} . \tag{10}$$

The contribution to the instantaneous inclusive and coincidence intensities from two atoms at r_i and r_j is, according to Eq. (4):

$$I_{ij}(R_l, t) = 2E_0^2 \left\{ 1 + \cos\left[k_l(d_1 - d_2) + \delta(t)\right] \right\}, \quad l = 1, 2 \tag{11}$$

$$\begin{aligned} I_{\Pi}(R_1, R_2, t) =& I_{ij}(R_1, t)\, I_{ij}(R_2, t) \\ =& \left(2E_0^2\right)^2 \Big\{ 1 + \cos[k_1(d_1 - d_2) + \delta(t)] + \cos[k_2(d_1 - d_2) + \delta(t)] \\ &+ \tfrac{1}{2} \cos[(k_1 + k_2)(d_1 - d_2) + 2\delta(t)] \\ &+ \tfrac{1}{2} \cos[(k_1 - k_2)(d_1 - d_2)] \Big\} , \end{aligned} \tag{12}$$

Again, it is necessary to average Eqs (11) and (12) over the observation time. Since in a chaotic source the two atoms radiate light independently of each other, $\delta(t)$ fluctuates randomly and all the terms depending on $\delta(t)$ vanish for the averaged intensities. The second order correlation function is then:

$$C^{(2)}(L) = 1 + \tfrac{1}{2} \cos\left[(k_1 - k_2)\alpha L\right] \tag{13}$$

and for N atoms distributed according to $\rho(r)$:

$$\begin{aligned} C^{(2)}(L) &= 1 + \frac{N-1}{N} \left|\tilde{\rho}[(k_1 - k_2)\alpha L]\right|^2 \\ &\approx 1 + \left|\tilde{\rho}[(k_1 - k_2)\alpha L]\right|^2 \qquad \text{for } N \gg 1 . \end{aligned} \tag{14}$$

If the field is coherent ($\delta(t)$ = constant) it makes no difference to take the average of the product of the intensities or the product of the averaged

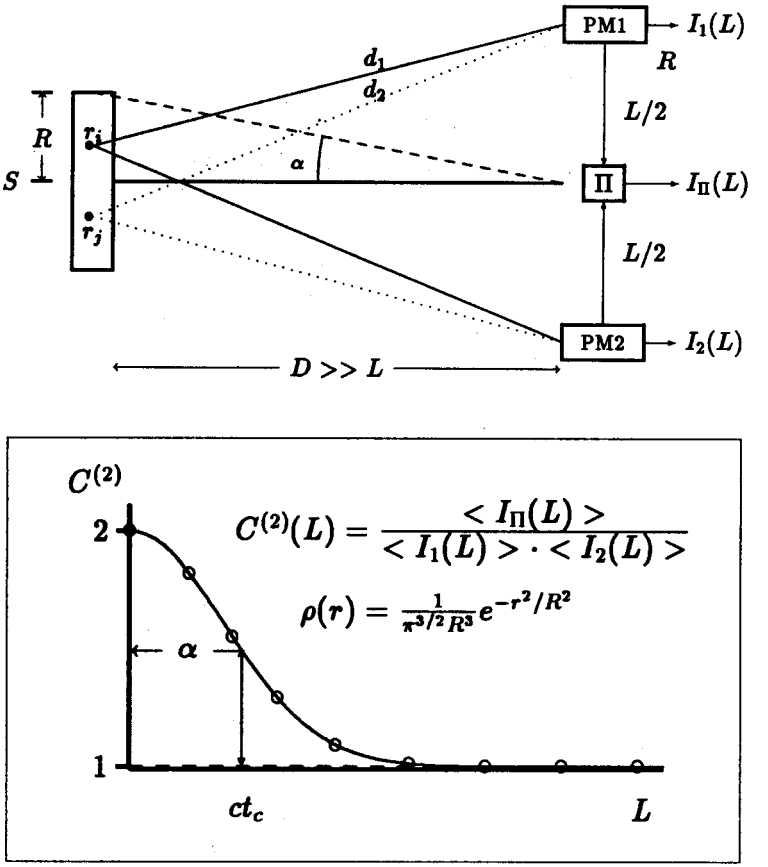

Fig. 4. Schematic set-up for the intensity interferometer and the correlation function for a Gaussian density distribution.

intensities. The numerator and denominator of Eq. (10) are, therefore, equal and the correlation function is equal to one.

As for the Michelson interferometer, the fall-off of the correlation function (Fig. 4) measures the angular size of distant light sources but with the fundamental difference that the field must no longer be coherent but chaotic instead.

Intensity interference is a new kind of interference since it is a multiparticle process and seems to contradict the fundamental dictum of Dirac [1]: "Each photon interferes only with itself. Interference between different photons never occurs." We shall see in the next section that quantum statistics provides the explanation for the occurrence of the intensity interference between identical particles.

The observation of first- and second-order interference effects can be summarized by introducing the notion of coherence. The term coherence is used to denote the correlation between the values of the field at two points separated in space or in time. The fact that there exist two kinds of correlation of first and second order leads us to distinguish also first- and second-order coherence. The fringes in the Young experiment are visible ($C^{(1)} > 1$) only if the field is coherent at least to first order and for the observation of intensity interference effects ($C^{(2)} > 1$) the field must be incoherent to second order whatever the first-order degree of coherence is. For a coherent field $C^{(2)} = 1$. The quantum theory of optical coherence can be found in reference [6].

4. Photon correlation in nuclear physics

In nuclear physics, identical particle correlations, a technique comparable to intensity interferometry, is a powerful tool to determine source sizes. The particles preferably used in this kind of measurement are those which are produced most abundantly in nuclear reactions: pions and kaons at ultrarelativistic energies to probe the fireball during the hadronization phase; protons, neutrons and complex particles at intermediate energies to probe the heavy ion collision zone at various stages of the reaction. Photons, the obvious probe for the study of interference phenomena, were never considered because of the difficulties in identifying them in the huge electromagnetic and hadronic background at ultrarelativistic energies or because of their weak production cross sections at intermediate energies. I will present in the following sections an experiment aimed at the determination of participant zone sizes by way of the measurement of the correlation between hard photons emitted in heavy ion collisions at intermediate energies.

Firstly, however, I will examine how the intensity interference effect arises in the correlation between identical particles.

4.1. Identical particle correlation

To construct the second order correlation function defined in Eq. (10), one needs to measure the coincidence rate between two detectors. The probability to detect two particles in coincidence is given by the modulus squared of the two-body wave function, ψ_{12}, which is in case of two emitters r_i and r_j:

$$\psi_{12} = \frac{1}{\sqrt{2}} \left\{ \psi_1(r_i)\psi_2(r_j) + \psi_1(r_j)\psi_2(r_i) \right\} . \tag{15}$$

The first term represents the amplitude for detecting the particle emitted from r_i in detector 1 and the particle emitted from r_j in detector 2. Since

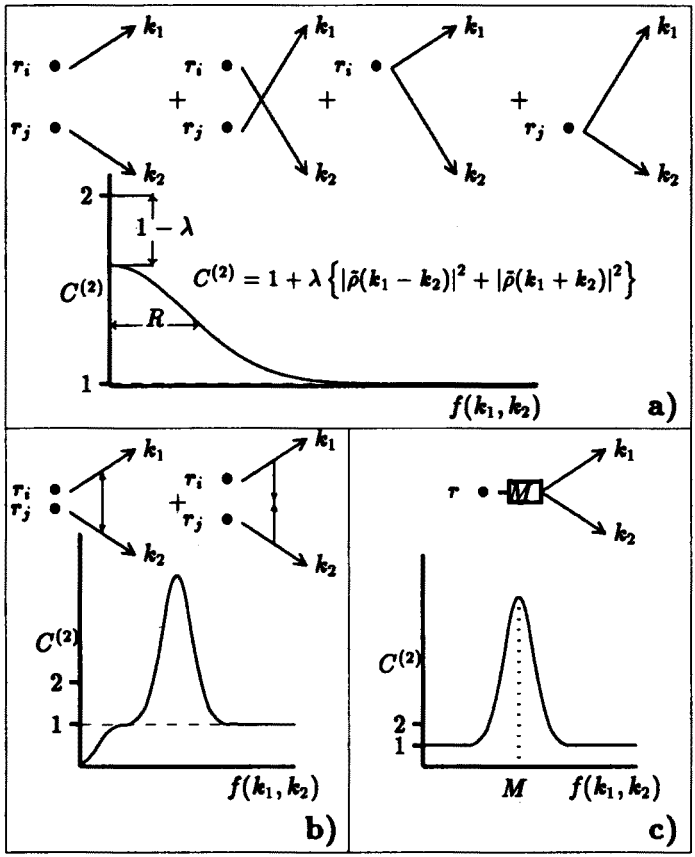

Fig. 5. Graphical representation of the mechanisms which generate a correlation between identical particles: a) the quantum statistics, b) final state interactions (Coulomb and nuclear), c) decay of a resonance of mass M.

the two particles are identical and therefore indistinguishable one needs to add the second term where the particles have been exchanged. If the particles are bosons the Bose–Einstein statistics requires that the two-body wave function is symmetric with respect to particle exchange, hence the + sign in expression (15). Otherwise, for fermions, the wave function is antisymmetric and the sign −. The two-body wave function (15) represents the two first contributions depicted in Fig. 5.a. The last two contributions where the particles are emitted from a single point are represented by the following wave function:

$$\psi_{12} = \frac{1}{\sqrt{2}} \left\{ \psi_1(r_i)\psi_2(r_i) + \psi_1(r_j)\psi_2(r_j) \right\} . \qquad (16)$$

Writing the single particle wave function in form of a plane wave, $\psi(r_i) = \exp(ikr_i)$, and assuming a density distribution, $\rho(r_i)$, for the points emitting particles in a source of radius R, the correlation function for the cases shown in Fig. 5.a) can be easily derived:

$$C^{(2)}(k_1,k_2) = \frac{\int \rho(r_1)\rho(r2)|\psi_{12}|^2\, dr_1 dr_2}{\int \rho(r_1)|\psi_1|^2\, dr_1 \int \rho(r_2)|\psi_2|^2\, dr_2}$$
$$= 1 + \tfrac{1}{2}\,|\tilde{\rho}(k_1 - k_2)|^2 + \tfrac{1}{2}\,|\tilde{\rho}(k_1 + k_2)|^2 \qquad \text{for } N = 2$$
$$= 1 + |\tilde{\rho}(k_1 - k_2)|^2 + |\tilde{\rho}(k_1 + k_2)|^2 \qquad \text{for } N \gg 1\,, \quad (17)$$

where N represents the granularity of the source. In contrast to astronomy, where the source size remains unchanged during the observation time, in nuclear physics the density distribution changes with time. Therefore, in Eq. (17), the 3-momenta must be replaced by the 4-momenta. Expression (17) is similar to the correlation function (14) with an additional term in $k_1 + k_2$, the total momentum of the two particles. This term is due to the case where the two particles are emitted from a single point. The full derivation of the correlation due to the quantum statistics can be found in Ref. [7].

Other processes can produce a correlation in the two-particle coincidence distribution. The first one, shown in Fig. 5.b), corresponds to the final state interactions between the two particles. This is the case of charged particles subject to the Coulomb and nuclear forces. The Coulomb force prevents the particles from being close to each other in phase space and results in a decrease in the correlation function at small relative momenta. The nuclear force is responsible for resonant states favoring strong correlation at the energy of the resonance. For photons the final state interactions are negligible, but one needs to consider the correlation due to the decay of unstable particles Fig. 5.a), such as neutral mesons into photons. The correlation function will be strongly enhanced at the mass of the particle.

For photons, the correlation function (17) must be changed to take into account their spin: left hand polarized and right hand polarized photons are not identical particles. Neuhauser [8] has shown that, under a number of conditions justified for nuclear bremsstrahlung photons, the correlation function is:

$$C^{(2)}(k_1,k_2) = 1 + \tfrac{1}{4}\left[1 + \cos^2\psi\right]\left[|\tilde{\rho}(k_1 - k_2)|^2 + |\tilde{\rho}(k_1 + k_2)|^2\right], \quad (18)$$

where ψ is the opening angle of the two photons. The effect of the polarization is to reduce the maximum value of the correlation function from 2 to 1.5 in the high energy limit ($\tilde{\rho}(k_1 + k_2) \sim 0$). Expression (18) is valid only in case where the photon production is isotropic. Razumov and Weiner [9]

have derived a more general expression taking into account the dynamics of the photon production and have shown that the maximum of the correlation function depends strongly on the angular distribution of the photons and can vary between 1.5 for isotropic emission and 2 for dipolar emission in the high energy limit.

4.2. Bremsstrahlung photons

High energy photons ($E_\gamma > 30$ MeV) have been extensively studied in the past decade for a large variety of systems over bombarding energies between 10 MeV/u and 124 MeV/u. The results are reviewed in references [10] and [11].

The global features are summarized in Fig. 6.

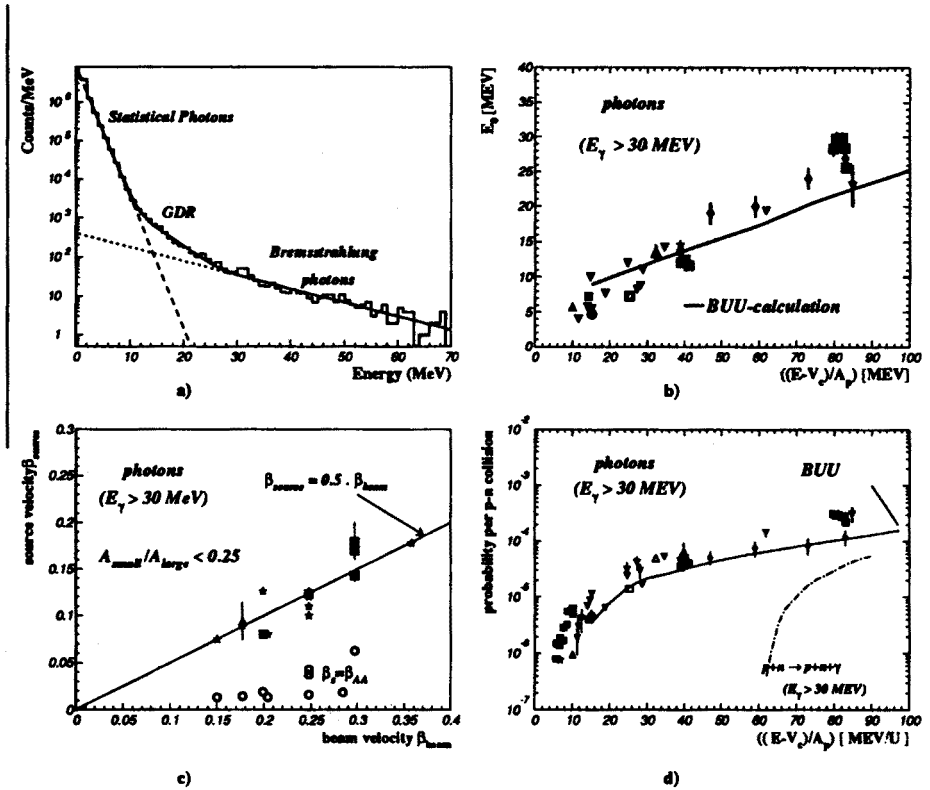

Fig. 6. Characteristics of the hard photons emitted in heavy ion reactions near the Fermi energy.

The hard photon spectrum, beyond the giant resonances region, exhibits an exponential shape Fig. 6.a) with an inverse slope parameter E_0 increasing with the bombarding energy Fig. 6.b). Exploiting the Doppler

shift, the velocity of the photon emitting source can be measured and is found to be equal to half the beam velocity Fig. 6.c). These observations lead one to identify the hard photons as the bremsstrahlung photons emitted in individual neutron-proton collisions. The production cross section can be expressed with only one parameter depending on the bombarding energy, the probability to produce a photon per neutron-proton collision:

$$P_\gamma = \frac{\sigma_\gamma}{\sigma_R \langle N_{np} \rangle_b}, \tag{19}$$

where σ_R is the total reaction cross section and $\langle N_{np} \rangle_b$ the number of neutron-proton collisions averaged over the impact parameter. The evolution of this probability with the energy available for the nuclear reaction is shown in Fig. 6.d) in comparison with the probability calculated in a free nucleon-proton collision. One observes that the photons with energies larger than 30 MeV can be produced in the medium well below the threshold energy of 60 MeV for a free collision. The additional energy necessary to create these sub-threshold photons is believed to be provided by the Fermi energy of the nucleons within the collision zone. Furthermore, phase space calculations indicate that, because of Pauli blocking, only first chance collisions participate in the production of hard photons.

To summarize, photons are produced through the bremsstrahlung mechanism in first chance individual neutron-proton collisions. Because of the stochastic nature of the collisions in a heavy-ion reaction, the total flux of photons results from an *incoherent* superposition of photons produced in individual collisions. We thus have at hand a chaotic light source which is well located in space, the participant zone, and in time, the duration of a nucleon–nucleon collision. The correlation technique may therefore be adapted for the determination of the spatial and temporal extent of the source using hard photons.

4.3. The two-photon correlation experiment

The experimental difficulties one needs to overcome in the measurement of the two-photon correlation function are: the unambiguous identification of the photons among the hadronic and cosmic-ray background and the weak production cross sections ($\sigma_{\gamma\gamma} \sim 10 \mu b$). One thus requires an efficient detection system with high angular and energy resolution and an effective background suppression (hadrons, e^+e^- conversion pairs, and cosmic rays). These problems were solved by the use of the photon spectrometer TAPS [1], an array of 320 hexagonal telescopes each consisting of

[1] Two Arms Photon Spectrometer, a GANIL-Gießen-GSI-KVI-Valencia coll.

a 2 mm thick NE102A ΔE detector and a 250 mm thick BaF_2 E detector. To optimize the collection of the electromagnetic shower induced by high energy photons the telescopes were assembled in 5 blocks of 64 detectors each, positioned around the target at an average distance of 60 cm. In the data analysis, the charged particles detected in TAPS, mainly protons and electrons, were rejected by using the information from the ΔE detector as a veto signal. In addition, photons and light particles were identified by using the difference in the pulse shape generated in the E detector and the different flight times. The residual contamination due to improperly identified hadrons was negligible. The energy and emission angle of the photons were obtained by reconstructing the electromagnetic shower. For 70 MeV photons, the final energy resolution was 3.5 MeV and the angular resolution was 1°. A detailed description of TAPS and the methods used to identify photons can be found in Refs [12–15]. We studied the system Kr+Ni at 60 MeV/u.

Experimentally, the second order correlation function defined by Eq. (10) is constructed as the ratio of the two-photon coincidence yield $Y_2(k_1, k_2)$ over an uncorrelated background generated by folding the single photon yields $Y_1(k_1)$ and $Y_2(k_2)$:

$$C^{(2)}_{\mathrm{exp}}(k_1, k_2) = \frac{Y_2(k_1, k_2)}{Y_1(k_1) \otimes Y_2(k_2)}. \tag{20}$$

$C^{(2)}$ is normalized to 1 in the region where the correlations are negligible. Cosmic-ray induced events recorded in random coincidence with the beam were eliminated in the analysis based on the shape of the shower [16] and left over conversion pairs or non continuous showers by setting a minimum relative angle of 18° between the two showers. In this way, 20,649 events were identified as two hard photon events. We estimate that the contributions from cosmic events not rejected (4 events over the whole spectrum) and from conversion pairs (6 events for invariant masses between 20 and 80 MeV) are negligible.

The correlation function is displayed in Fig. 7 as a function of the invariant relative momentum, $Q_{\mathrm{inv}} = \sqrt{-(k_1 - k_2)^2}$, which is equivalent for photons to the invariant mass. This kind of representation, commonly used in particle physics, has been selected because Q_{inv} allows one to easily identify the correlation originating from $\pi^0 \rightarrow 2\gamma$, as seen in the figure at $Q_{\mathrm{inv}} = 135$ MeV. The neutral pion contribution to the correlation function has been calculated with the help of a GEANT Monte Carlo simulation (dashed line) indicating that it is negligible at low invariant mass. Therefore, below 60 MeV, the spectrum contains mainly bremsstrahlung photons and the rise towards low Q_{inv}, in the interval from 40 MeV down to 5 MeV, is attributed to the expected interference effect between photons.

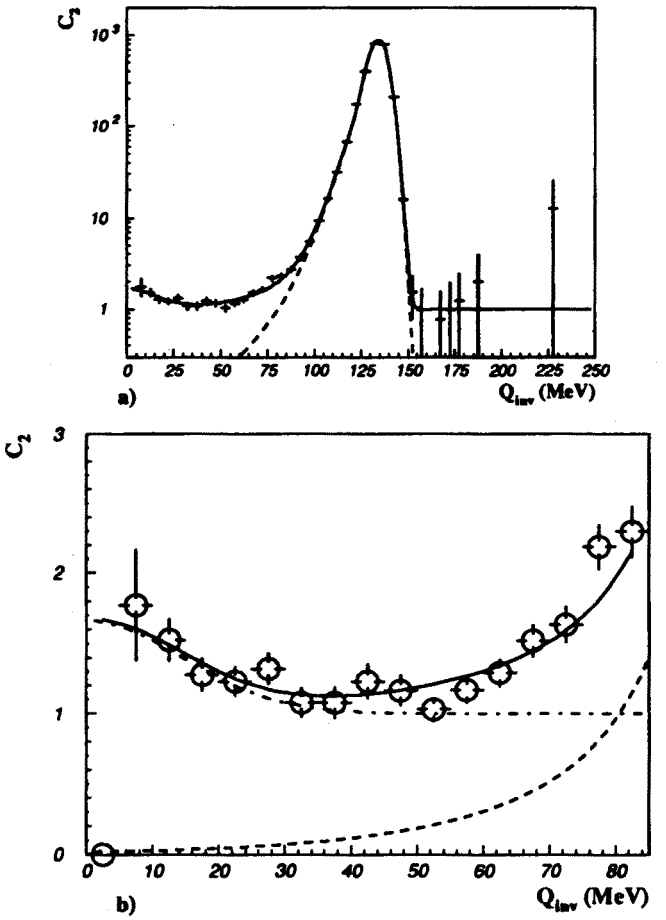

Fig. 7. Correlation function measured for hard photons from the system Kr+Ni at 60 MeV/u. Subfigure b) is an enlargement of subfigure a) at low invariant mass. The solid line is a fit to the data using Eq. (22), the dashed line shows the π^0 contribution, and the dot-dashed line shows the interference effect.

The following expression was fitted to the experimental correlation function:

$$C^{(2)}_{\mathrm{exp}}(Q_{\mathrm{inv}}) = K_0 + K_1 \cdot g_{\gamma\gamma}(Q_{\mathrm{inv}}) + K_2 \cdot g_{\pi^0}(Q_{\mathrm{inv}} - m_{\pi^0}), \qquad (21)$$

where K_0 is a coefficient used to normalize the correlation function to unity for uncorrelated photons and the last term describes the contribution from the neutral pions. The interference term $g_{\gamma\gamma}$ is obtained by assuming that the source density distribution is of gaussian shape with a width R_{inv} and

by neglecting the second term of Eq. (18) ($\tilde{\rho}(k_1 + k_2) \sim 0$ for $k_{1,2} \gg 1$). The interference term thus has the following form:

$$C^{(2)}(Q_{\mathrm{inv}}) = 1 + \lambda \cdot \exp\left(\frac{Q_{\mathrm{inv}}^2}{2\sigma_c^2}\right), \tag{22}$$

where $\sigma_c = \hbar c / R_{\mathrm{inv}}$ is the correlation length and $\lambda = K_1/K_0$ is a factor which represents the reduction of the correlation function at zero relative momentum due to the spin of the photons, to the dynamics of their production (see section 4.1), to the partial coherence of the source and chance coincidences. We assumed that this parameter is a constant. The result of the fit is shown in Fig. 7 as the solid line. The maximum of the correlation function at zero relative momentum is equal to 1.7 ± 0.2, consistent with the predicted values (see Section 4.1). The correlation length is equal to 15 ± 3 MeV corresponding to an invariant gaussian radius equal to 13 ± 3 fm and to an equivalent hard sphere radius equal to 20 ± 4 fm. The size calculated for the photon source considering an average impact parameter of 3.5 fm and an average number of participants equal to 76 nucleons is found equal to $R = 5$ fm. The measured photon source size is thus 4 times larger than the size of the expected participant zone, although it must be realized that R_{inv} includes both the spatial and temporal dimensions. We don't have yet an interpretation for this unexpected observation.

5. Summary

The global features observed for the production of hard photons in heavy-ion collisions in the vicinity of the Fermi energy indicate that the photons are predominantly produced in first chance individual nucleon-nucleon collisions. The photon source is therefore chaotic and well localized in space and time. All the required conditions are thus met to measure the intensity interference effects which depend on the dimensions of the photon source. The principles of this method have been described and the correlation function between identical particles, in particular photons, has been derived.

The results of an experiment performed using the photon spectrometer TAPS have demonstrated that it is possible to measure and identify two-photon events originating from the bremsstrahlung radiation emitted during the collisions between participant nucleons. It was shown that the strong correlation due to the decay of neutral pions does not mask the second order interference effect. Whereas the effect was seen in the data the interpretation of the measured source size remains an open question. Why is the source size so much larger than the expected size of the participant zone? Do we really observe the interference effect or is it another trivial effect? What are the respective roles of the spatial and temporal extent of the

source? With the present data it is not possible to answer these questions. Certainly new experiments are needed. One could, for example, repeat the experiment using a much heavier system at the same bombarding energy to check if the correlation function is narrower as expected for a larger source size. The ultimate dream would be to collect enough data (that means a lot!) to be able to disentangle the spatial and temporal extent in a bidimensional representation of the correlation function, relative energy versus relative momentum.

I would like to thank my colleagues in the TAPS collaboration who have carried out the major portion of the acquisition and analysis of the data included in this contribution – in particular M. Marqués, T. Matulewicz, F. Lefèvre, and P. Lautridou. In addition I wish to aknowledge many fruitfull discussions with R. Ostendorf and J. Québert. I thank N. Orr for assistance in the preparation of the manuscript.

REFERENCES

[1] P.A.M. Dirac, *The principles of quantum mechanics*, Oxford, London, 1958, 4th ed., p. 9.
[2] A. Tonomura, J. Endo, T. Matsuda, T. Kawasaki, *Am. J. Phys.* **57**, 117 (1989).
[3] R. Hanbury-Brown, R.Q. Twiss *Phil. Mag.* **45**, 663 (1954).
[4] G. Goldhaber, S. Goldhaber, W. Lee, A. Pais, *Phys. Rev.* **120**, 300 (1960).
[5] J. Québert, *Ann. Phys. Fr.* **17**, 99 (1992).
[6] R.J. Glauber, *Phys. Rev.* **120**, 2529 (1963);R.J. Glauber, *Phys. Rev.* **131**, 2766 (1963).
[7] M. Gyulassy, S.K. Kauffmann, L.W. Wilson, *Phys. Rev.* **C20**, 2267 (1979).
[8] D. Neuhauser, *Phys. Lett.* **B182**, 289 (1986).
[9] L.V. Razumov, R.M. Weiner, in Proccedings of the II Workshop on Physics Related to TAPS, Guardamar, Spain, 1993, to be published.
[10] W. Cassing, V. Metag, U. Mosel, K. Niita, *Phys. Rep.* **188**, 363 (1990).
[11] H. Nifenecker, J.A. Pinston, it Prog. Part. Nucl. Phys. **23**, 271 (1989).
[12] R. Merrouch, Thèse Université de Caen, Ganil Report T-91-01, 1991.
[13] P. Lautridou, F. Lefèvre, M. Marqués, T. Matulewicz, R. Ostendorf, J. Québert, Y. Schutz, *Nouvelles du GANIL* **44**, 29 (1993).
[14] M. Marqués, P. Lautridou, F. Lefèvre, G. Martínez, T. Matulewicz, R. Ostendorf, J. Québert, Y. Schutz, *Nouvelles du GANIL* **45**, 45 (1993).
[15] R. Ostendorf, Thèse Université de Caen, Ganil report T-93-03, 1993.
[16] T. Matulewicz, P. Lautridou, F. Lefèvre, M. Marqués, R. Ostendorf, J. Québert, Y. Schutz, *Nouvelles du GANIL* **45**, 33 (1993).